PJEST

Insight on Mg-doping dependent structural, electronic and optical properties of $CaTiO_3$ for solar cell applications: A DFT study

Nida Khan[1], Muhammad Bilal Tahir[1, 2], Bilal Ahmed[1*], M. Sagir[3]

[1]Institute of Physics, Khwaja Fareed University of Engineering and Information Technology, Rahim Yar Khan, Punjab, Pakistan
[2]Centre for Innovative Material Research, Khwaja Fareed University of Engineering and Information Technology, Rahim Yar Khan, Punjab, Pakistan
[3]Institute of Chemical and Environmental Engineering, Khwaja Fareed University of Engineering and Information Technology, Rahim Yar Khan, Punjab, Pakistan
*Corresponding Author: raisbilalahmed@gmail.com

Citation: Nida Khan, Muhammad Bilal Tahir, Bilal Ahmed, & M. Sagir. (2025). Insight on Mg-doping dependent structural, electronic and optical properties of CaTiO3 for solar cell applications: A DFT study. Pakistan Journal of Emerging Science and Technologies,

https://doi.org/10.5281/zenodo.17758868

Academic Editor: Dr. M. Javaid Afzal

Received date: 24-03-2025
Revised date: 03-10-2025
Accepted date: 04-10-2025
Published date: 03-12-2025

ABSTRACT: We used first-principles density functional theory (DFT) computations to carefully study the structural, electrical, and optical characteristics of pure and Mg-doped $CaTiO_3$. In contrast to prior studies that concentrated on the dielectric or surface properties of $CaTiO_3$, the current research investigates the microscopic process by which Mg substitution alters the band structure and optical response pertinent to solar energy conversion. Our findings indicate that the addition of Mg results in a marginal decrease in both lattice parameters and bond lengths, alongside an increase in the electronic band gap from 1.85 to 2.05 eV, signifying a blue shift advantageous for solar cell performance. The movement of the Fermi level into the valence band and the changes in the partial density of states show how strongly Mg affects the electrical structure of $CaTiO_3$. The optical absorption edge also moves closer to the visible region, which suggests that the optoelectronic response is better. This study offers novel theoretical perspectives on band gap engineering via Mg doping in $CaTiO_3$ and illustrates its viability as a cost-effective and eco-friendly material for next-generation solar and optoelectronic devices.

Keywords: CASTEP, Opto-electronic, electronic parameters, di-electric function, density functional theory.

1. Introduction

A significant and promising renewable resource is solar energy [1]. The direct conversion of light into electricity through photoelectric conversion means that it has the potential to completely replace fossil fuel energy without having negative effects on the environment [2]. People must focus on clean energy in order to stop environmental contamination [3]. An important concern revolves around the excessive utilization of fossil fuels, leading to a rise in greenhouse gas levels in the atmosphere and contributing to climate change [4]. These days, the global movement towards the investigation of clean, energy-efficient sources depends on photovoltaic technology [5].

Despite the fact that there is an increase in the percentage of photovoltaic results in this scenario, the power conversion efficiencies that are recorded are much lower than the levels that were predicted. Furthermore, it remains difficult to achieve the corresponding

theoretical limits [6, 7]. This is mostly caused by problems arising from different factors, like losses during the recombination process, difficulties in maintaining consistency, not-so-ideal alignment of energy bands, and poor overall quality of the material due to challenges in growing a uniformly distributed single-phase quaternary material [7-9]. However, when the alignment is not ideal, it can lead to less efficient electronic processes, impacting the overall performance of the material, such as in electronic devices like transistors or solar cells. Because of these challenges, researchers are currently focusing their efforts on the discovery of novel binary semiconducting constituents that possess a high possibility of reconciling the gap between efficient conversion, affordability, and environmental friendliness. This is because these substances have the potential to bridge the gap between these three factors [10]. In this context one of the most important oxides in solid-state physics, $CaTiO_3$, has been the subject of numerous studies examining its structural and physical properties [11]. The general formulation for perovskites is ABX_3, here A and B represent different types of atoms positioned at the corners and center of the cubic crystal lattice, respectively. Meanwhile, the X atom is situated at the center of the faces of the lattice (Wang, Huang, Wu, & Chen, 2021). Due to its outstanding characteristics, interest in ($CaTiO_3$) perovskite is growing over time [12]. Minimal expense, innovative prerequisites, and economy are the primary powers behind the development of novel materials for this species [13]. $CaTiO_3$ is a ferroelectric perovskite that has a flexible structure and exhibits dielectric behavior for transitions and microwave device application. Changes in pressure and temperature have an impact on its phase transition and electrical properties of metal [14]. CaTiO3's electrical and optical properties can be improved by expanding a dopant at a cation or anion, which changes the band hole [13]. These resources are crucial for basic research as well as their technological applications [15]. Cockayne et al. and Wang et al. also carried out first principles computations of $CaTiO_3$, however they mainly concentrated on the dielectric constant, optical characteristics, and surface structures [16]. The primary causes of the widespread research on perovskites are their wide band gap and low-temperature distortion. These gained popularity as a result of phase (Luo et al., 2020). Perovskites contain several fascinating characteristics, include as superconductivity, high dielectric constants, and superior electrical transport characteristics [17]. Their usage as photoactive materials is constrained by broadband and gap, particularly in solar energy conversion devices [18]. Under UV rays, pure $CaTiO_3$ transforms, while under visible light, Cu-doped $CaTiO_3$ undergoes a reaction with a high photocatalytic activity [19]. Calcium titanate is frequently utilized in photocatalysis, biomedical green-screen displays, fiber-optic communication amplifiers, optoelectronic devices, and solid-state laser display imaging [20]. Because of the continuous interest for novel phosphor materials as little light sources and photonic gadgets to obtain short frequency sources that can be siphoned with diode lasers, these aftereffects of perovskites-type structures have revived the investigation of their glowing

processes (Oliveira et al., 2015). As a result of their flexible purposes in the field of optoelectronic gadgets, cordial climate, and notable compound soundness for utilization in white-light-radiating LEDs (wLEDS) devices, $CaTiO_3$ doped LEDs earth (RE) ions have garnered a lot of interest[21]. First rule estimations, which depend on thickness practical hypothesis, were utilized to compute specific boundaries of the framework being talked about. This method is beneficial for gaining a better knowledge of Mg doping in $CaTiO_3$ at the microscopic level [13]. The impetus for incorporating Mg into the $CaTiO_3$ lattice stems from the necessity to address the inherent constraints of pure $CaTiO_3$, namely its comparatively wide band gap and modest charge carrier mobility, which impede its efficacy in solar energy conversion. Because Mg is a lighter alkaline-earth element with a smaller ionic radius than Ca, it can replace Ca in the lattice and change the local electrical environment by causing strain. It is thought that this change will change the band structure, make the energy levels line up better, and improve optical absorption in the visible range. Also, adding Mg can help separate charge carriers better and cut down on recombination losses, which would improve the overall performance of photoelectronic devices. So, looking into how adding Mg affects $CaTiO_3$'s electrical and optical properties is a good way to make it work better for high-efficiency solar cells and other optoelectronic uses.

We utilized first principle calculations to investigate the optical, electronic, and structural properties of innovative ternary $CaTiO_3$ structures for solar cell applications. While there has been a lot of research on perovskites based on $CaTiO_3$, most of it has been about their optical, dielectric, or surface properties. There hasn't been much focus on how to change their composition for solar energy applications. The specific microscopic mechanism through which Mg doping alters the electronic structure and optical response of $CaTiO_3$ is still largely unexamined. Consequently, this study seeks to address this deficiency by methodically examining the structural, electronic, and optical properties of Mg-doped $CaTiO_3$ through first-principles calculations. This work offers novel insights into the impact of Mg substitution on band gap modulation, charge redistribution, and light absorption characteristics, which are critical factors influencing the photovoltaic performance of perovskite materials. The results help design materials that are cheap and good for the environment for use in next-generation solar cells.

2. Method of calculations

The calculations were completed utilizing CASTEP, which is a thickness useful hypothesis (DFT) implementation (Prentice et al., 020). The calculation was utilized to do the estimations for the design taking. As per Perdew-Burke-Ernzerhof, the trade connection particle energy term has been assessed utilizing summed up angle guess (GGA), which considers the slope in the charge thickness across the crystal (Iasir and Hammond, 2020). The chosen structure for $CaTiO_3$ is the ideal cubic arrangement, falling

within the space group pm-3m. This selection is based on the stability of this structure, particularly at room temperature at this structure, the Ca^{+2} metal, which is bigger, is located at the corners of the cube, while the Ti^{+4} metal, which is smaller, is located in the middle of the body. Together, these two metals are surrounded by oxygen atoms at the face centers inside the unit cell.

The number of atoms in a normal cubic unit cell of $CaTiO_3$ was increased by expanding it to a 2 × 2 × 1 supercell, resulting in a total of 42 atoms. During the introduction of Mg into $CaTiO_3$ by substituting one Ca atom, the geometric analysis of the supercell resulted in the doping of two atoms following the optimization procedure. A Monkhorst-Pack grid with dimensions of 2x2x1 was used to calculate Brillouin zone interactions. The cut off energy of the system was kept at 324.42 eV.

3. Results and Discussion

3.1. Structural properties

Lattice parameters of $CaTiO_3$ are as a =7.781 Å. These boundaries show a well-disposed connection with detailed determined results (a=7.788 Å). The disparity in cross-sectional boundaries between our computed and reported results reduced by 0.007 Å after incorporating correlation analysis, demonstrating the precision of our outcomes. Introducing 10 Mg particles at the Ca site resulted in a subtle alteration in the grid boundaries. The expansion of Mg causes a reduction in the consistent cross-sectional dimensions (for example a = 7.515 Å, b =, 7.607 Å, and c, = 7.507 Å) [22]. In comparison, to Ca the lower radii Mg is responsible for this change (Mg = 1.6 Å and Ca = 1.97 Å).

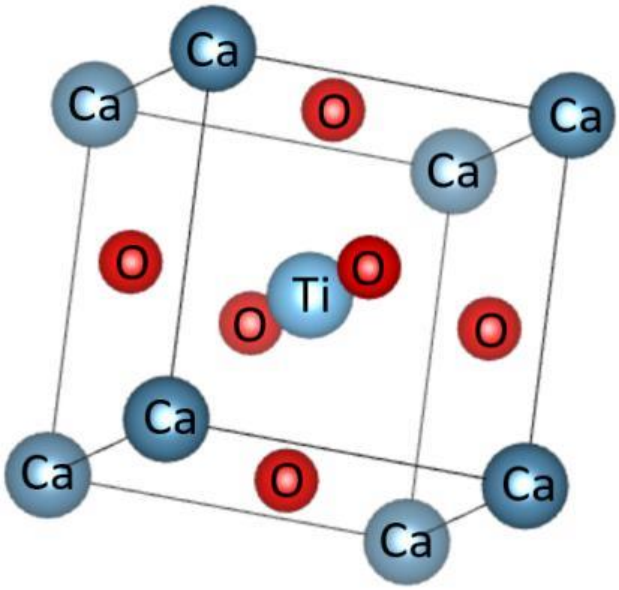

Fig 1: Optimized cell (space group 221 pm3m) of cubic $CaTiO_3$

In assessing the thermodynamic stability of $CaTiO_3$ compounds, the determination of formation energy (E_{form}) is crucial. Formation energy represents the energy needed to arrange the molecules within a composite. The relationship given below is used to determine formation energy.

$$E_{form} = E_{(CaTiO3)} - (E_{Ca} + E_{Ti} + 3E_O) \quad (1)$$

where, $E_{(CaTiO3)}$ is the total energy of $CaTiO_3$, E_{Ca}, E_{Ti} and E_O are the overall energy of the atom in bulk form, the value of formation energy for $CaTiO_3$ is -39.82 eV. The negative sign in the value of formation energy shows the stability of the compound and it can be synthesized in laboratory.

3.2. Electronic properties

The most significant energy peak in the valence band and the lowest energy peak in the conduction band are critical for establishing the band gap. To understand the conductivity of a particular material, the band gap is indispensable. It is generally called the energy gap; electrons don't remain for a surprisingly long time in this state. When the major peak of the valence band and the peak of the conduction band overlap on a line that is comparable to one another, a direct band gap is found. In contrast, an indirect band gap occurs when these energy levels are not aligned. The structure of band is an imperative variable to obtain processed data about conceivable energy ranges for involved and empty electrons, as well as the movement of valence electrons to the conduction band [23]. The structure of band for $CaTiO_3$ is illustrated in Fig. 2(a). The significant energy levels in the valence band manifest at the Z point, whereas the lowest energy levels in the conduction band are situated at the G point. This difference creates a band gap of 1.857eV, commonly acknowledged as the material's band gap. This value suggests an indirect band nature. This band gap becomes more significant when analyzed and reported. The transition of electrons from the valence band to the conduction band results in the dissipation of energy due to the indirect nature of the band gap. Figures 2(b-d) depict the observed evolution of 0.11%, 0.33%, and 0.55% Mg-doped $CaTiO_3$. The Z point is where the peaks of the valence band take place, whereas the G points are where the troughs of the conduction band are situated. Due to the fact that they are not located at the same place, the band gap is classified as indirect and measures 2.055 eV for the maximal dopant. The observed band gap exhibits a lower value when contrasted with the reported data.

Following Mg doping, the Fermi level shifts away from the conduction band and the band gap appears. The band gap increases after doping compared to the band gap of pure $CaTiO_3$ [24]. The TDOS and PDOS were calculated to gain insight into the modifications in the band structure after doping with Mg.

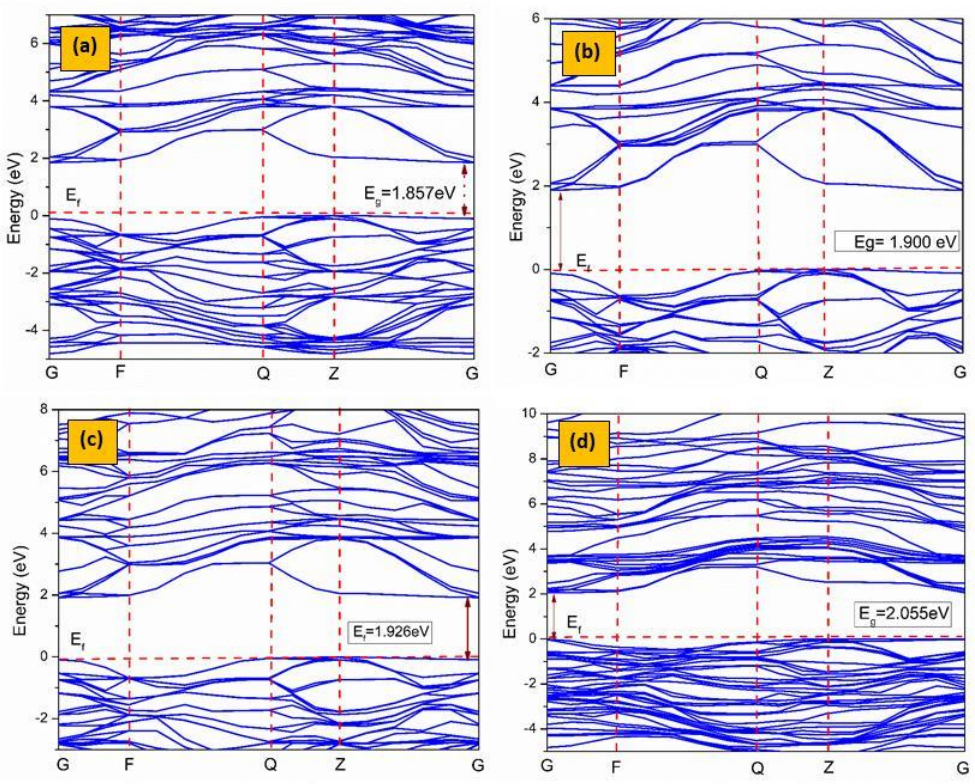

Fig 2: Band structure of (a) pure $CaTiO_3$ (b) 2-atoms doped (c) 6-atoms doped (d) 10-atoms

Table 1. Lattice parameters and band gap of pure and Mg-$CaTiO_3$

Material/doping	Optimized Lattice parameters (Å)	Band gap E_g (eV) Previous work	Band gap E_g (eV) Recent work
$Mg_xCa_{1-x}TiO_3$ x = 0	7.781	1.84 [13]	1.857
$Mg_xCa_{1-x}TiO_3$ x = 0.11	7.733	---	1.900
$Mg_xCa_{1-x}TiO_3$ x = 0.33	7.652	---	1.926
$Mg_xCa_{1-x}TiO_3$ x = 0.55	7.515	1.92 [25]	2.055

The comparison between virgin $CaTiO_3$ and $CaTiO_3$ doped with Mg regarding the PDOS and TDOS (a-e) is shown in Fig. 2. In PDOS, D-states have more pronounced characteristics than other states (e.g., s-states or p-states). Fig. 2 shows the analysis of pure and Mg-doped CaTiO3 to visually display PDOS. Doping with pure Mg shows a significant change in the valence band (VB) and conduction band (CB) states as seen in these graphs. Though having a smaller peak, the d-states of the CB get sharper as the dopant concentration rises post-Mg doping. PDOS shows clear changes in the CB and VB peaks brought on by magnesium. In a doped system, s-states play a crucial role in the valence band, while d-states take part to the conduction band, diverging from a pristine system. In the case of Ca, the presence of Mg as a dopant exerts a noticeable influence. The primary impact of magnesium is observed on oxygen, specifically on adjacent atoms [26]. On the TDOS diagram, the influence of Mg-doping is immediately apparent. The peak of the valence band ranges from -15eV to -22eV due to the newly discovered states of Mg. The energy peaks of the conduction band fall within the ranges of 2eV to 8eV. As the top peaks of the VB and the bottom of the CB are not aligned, the resulting band gap is indirect. In a doped system, s-states dominate the valence band, while d-states govern the conduction band, which contrasts with a pure system. Mg-doping significantly impacts Ca, particularly affecting oxygen or nearby atoms. The observed effects of Mg-doping on TDOS reveal states of magnesium, with the valence band peak in this chart situated between -15eV and -22eV, while the CB energy peaks are within the range of 2eV and 8eV.

Adding Mg to the $CaTiO_3$ lattice creates localized electronic states that change the hybridization between Ti–O orbitals a little bit. As seen in the band structure and density of states plots, this change makes the band gap wider and moves the Fermi level up toward the valence band. The larger band gap means that electronic states are more

localized which lowers recombination losses and improves charge carrier separation. These are important for good photovoltaic performance. The movement of the Fermi level also shows that the concentration of carriers and the potential barrier at interfaces have changed. This can make it easier for charge to move through device architectures. These electronic changes caused by Mg doping help change the optoelectronic properties of $CaTiO_3$, making it a better and more stable material for solar energy conversion and optoelectronic uses.

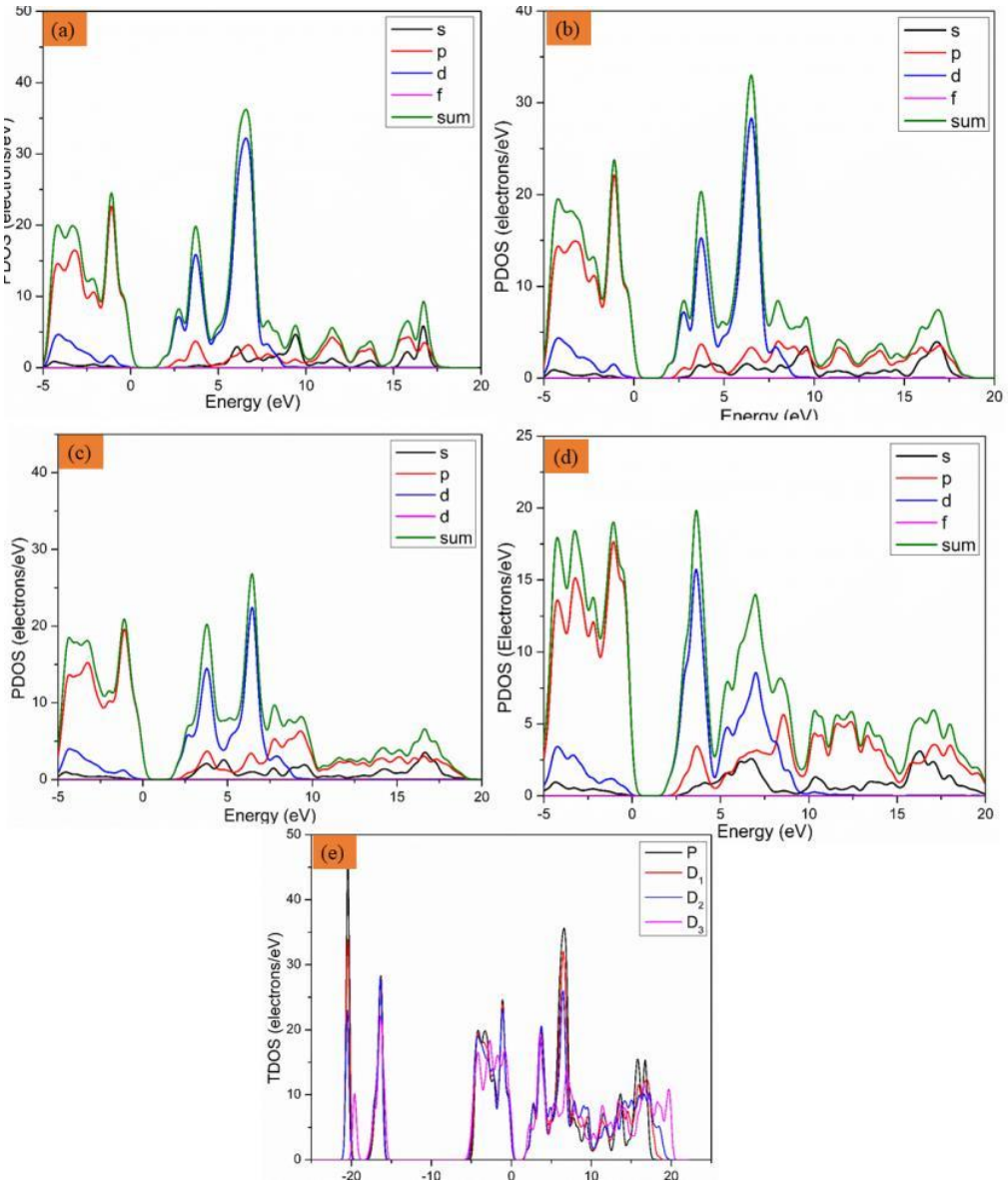

Fig 3: PDOS of (a) Pure $CaTiO_3$ (b) 2-atom doped (c) 6-atom doped (d) 10-atom doped (e) TDOS of $CaTiO_3$

3.3. Optical properties

Given that $CaTiO_3$ is a commonly utilized semiconductor due to its electrical band structure, we look at how Mg-doping affects this material. Optical attributes provide essential information about the interaction between light and materials. Prior to investigating the effects of Mg-doping on the characteristics of the original material, we evaluate each of these optical qualities for the material without any doping. Figures 4 and 5 provide a contrast in the optical characteristics of the pure system and the system doped with magnesium. The optical parameters that have been described are interrelated and vary depending on the frequency. It is essential to use sophisticated dielectric functions to understand the behaviour of these optical characteristics [27]. The optical characteristics of both pure and doped $CaTiO_3$ are ascertained utilizing the formula [28] and depicted in Figures 4&5.

$$\varepsilon(\omega) = \varepsilon_1(\omega) + i\varepsilon_2(\omega) \quad (2)$$

$$n(\omega) = [\, \varepsilon_1(\omega)/2 + \{\, \varepsilon_1^2(\omega) + \varepsilon_1^2(\omega) \,\}^{1/2} /2 \,]^{1/2} \quad (3)$$

$$L(\omega) = -\, I'm\, (\, \varepsilon(\omega)^{-1} \,) = \varepsilon_2(\omega) / \varepsilon_1(\omega)^{\,2} + \varepsilon_2(\omega)^{\,2} \quad (4)$$

$$I(\omega) = 2^{1/2}\omega\, [\{\varepsilon_1^{\,2}(\omega) + \varepsilon_1^{\,2}(\omega)\,\}^{1/2} - \varepsilon_1(\omega)\,]^{1/2} \quad (5)$$

$$R(\omega) = (n + ik - - 1) / (n + ik + 1) \quad (6)$$

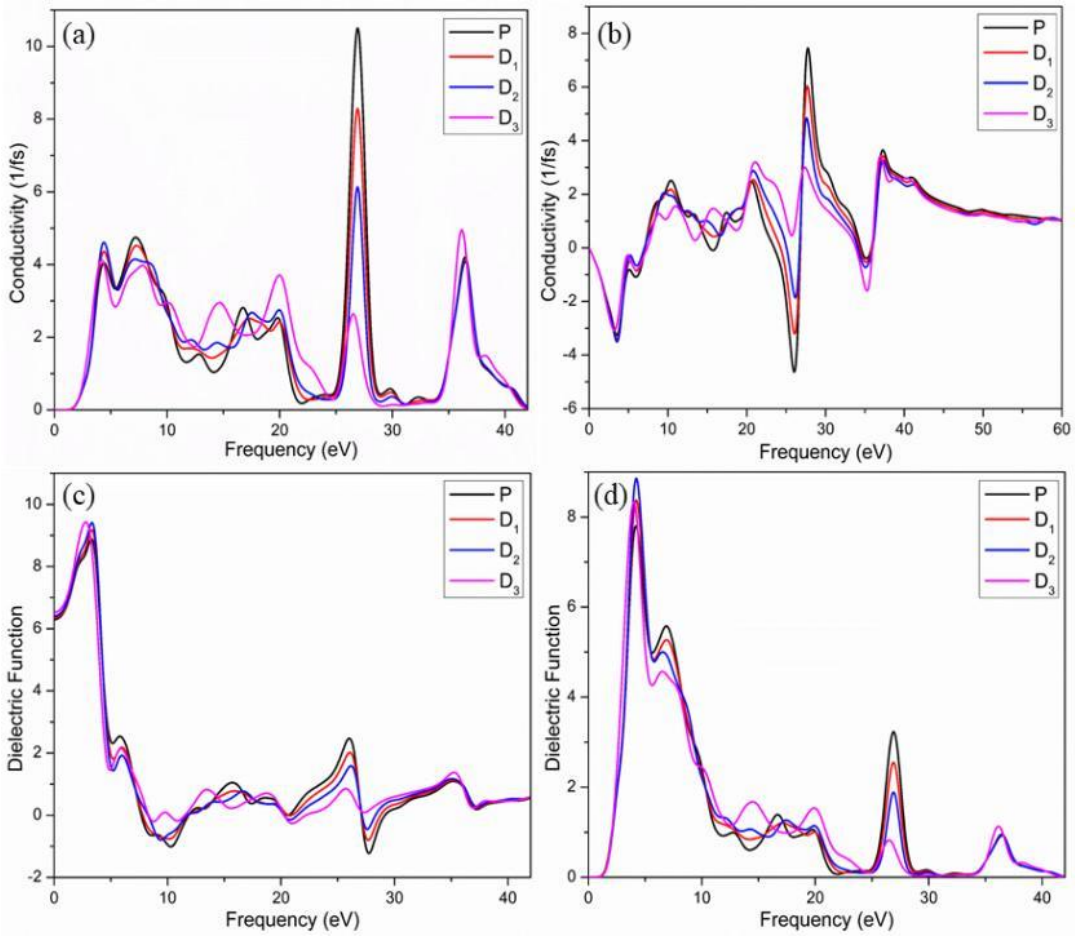

Fig 4: (a) The real (b) imaginary part of the conductivity (c) the real (d) the imaginary part of the Dielectric function of pure and Mg-doped $CaTiO_3$

Indeed, this is essential to analyze all optical characteristics, and complex dielectric functions show a crucial role in defining these optical characteristics. Additionally, complex dielectric functions are valuable for describing how a material responds as it interacts with external influences [29]. The dielectric function comprises two components: a real component and an imaginary component, as illustrated in Fig. 3(c, d). The real component specifies the energy value at which electro-excitation occurs, representing polarization. Meanwhile, the imaginary component provides details about absorption at a specific wavelength [29]. The graph clearly illustrates that the imaginary component of the dielectric function for the pure system reaches its lowest point at 0 eV, suggesting that absorption in pure $CaTiO_3$ is minimal at this energy level. Four prominent crests in the imaginary component of the dielectric function, observed at energy levels of 4.3 eV, 6.8 eV, 26.9 eV, and 36.4 eV, become apparent as the photon energy increases from 1.5 eV. These peaks closely correspond to the absorption peaks observed in Fig. 5 (c) at the same energy levels.

At 4.6 eV, 27.5 eV, and 36.7 eV, significant peaks manifest in the Fig 5 (b) of the dielectric function within the doped system which are strongly associated with absorption peaks at the same energy levels. In the doped system, the most prominent absorption peak occurs at 36.5 eV and subsequently decreases. It is noteworthy that the introduction of Mg in the doped system not only reduces the sharpness of the peaks post-doping but also shifts the absorption peaks towards lower energy levels. When light interacts with electrons confined to their lattice locations, plasma oscillations occur. In contrast to pure $CaTiO_3$, the distinct peaks of plasma oscillations in Mg-doped systems shift toward lower energy levels. The loss function maxima for the pure and doped systems are compared in Fig. (d). A major feature of semiconductors is shown to be the relationship between the lowest values of the imaginary component of the dielectric function and the loss function. Figure 5 (c, e) illustrates the inverse relationship between absorption and reflection when the absorption coefficient is at its minimum and the loss function value is at its maximum.

As a result, the introduction of Mg-dopant alters the absorption spectra. The Mg-doped system exhibits a lower refractive index than the pure system, ranging from 1.5 to 1.7, respectively, with the highest refractive index occurring at 4.6 eV. The refractive index value decreases as absorption increases, as depicted in Fig. 5(c). The findings from this study affirm that Mg improves/increases the optical characteristics of pure CaTiO3. The blue shift in the absorption spectra that was seen when Mg was added shows that the optical band gap of $CaTiO_3$ has gotten bigger. This change shows that adding Mg changes the electronic structure in a way that makes it easier for higher-energy photons to be absorbed in the visible range, which improves the efficiency of light harvesting. Adjusting the band gap in this way is good for improving the spectral response and lowering non-radiative recombination losses in devices that convert solar energy. As a result, the Mg-doped $CaTiO_3$ system has better charge carrier separation and transport properties, which can improve the overall power conversion efficiency of perovskite solar cells made of $CaTiO_3$.

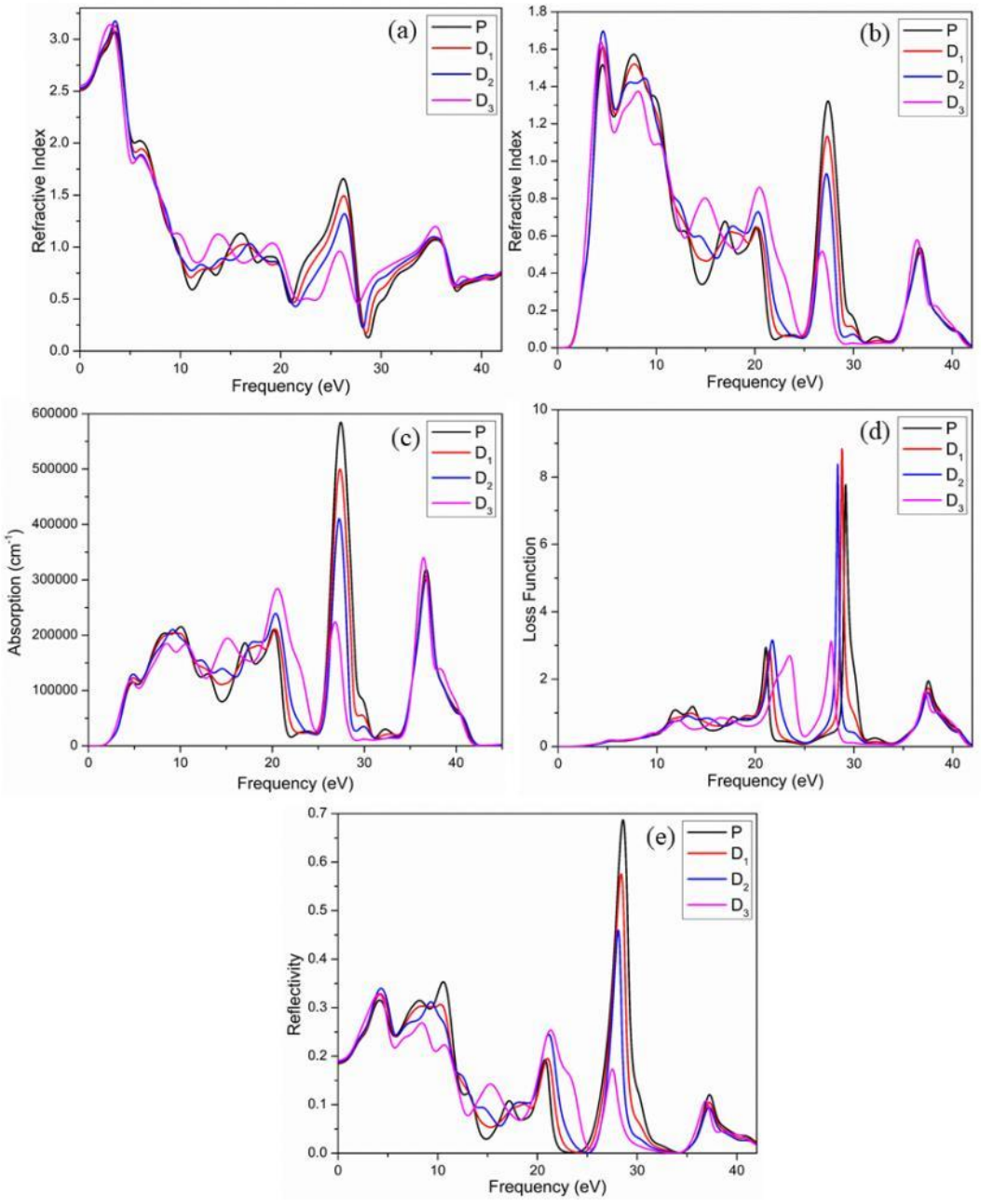

Fig 5: (a) The real (b) and the imaginary part the of the refractive index (c) Absorption (d) Loss function and (e) Reflectivity of pure and Mg-doped $CaTiO_3$

Conclusion

In this study, we directed a systematic examination into the influence of Mg doping on the structural, optical, and electronic characteristics of both pure and doped-CaTiO3 using the CASTEP module. Our analysis included an exploration of the relationship between structural changes and electronic characteristics induced by Mg doping. Using

TDOS and PDOS profiles, we particularly investigated the electronic band gap of both the pure and Mg-doped $CaTiO_3$, clarifying the band gap characteristics. Mg doping caused the Fermi level (Ef) to move toward the valence band (VB), which opened the band gap, as seen by the band structure diagrams. The movement of Ef toward the VB, together with a larger band gap, suggested a stronger interaction between Mg and its adjacent particles. Especially notable were the changes in the PDOS of O-2s at the lower end of the VB following Mg doping; the O-2p at the top of the conduction band (CB) also underwent modifications. The observed increase in the band gap, particularly beneficial for solar cells and semiconductor devices, was confirmed through the blue shift observed in the absorption spectrum. This shift further highlighted the enhanced band gap resulting from Mg doping, demonstrating its potential applications in optoelectronic and semiconductor technologies.

For future research, the experimental synthesis and characterization of Mg-doped $CaTiO_3$ utilizing sol–gel or solid-state reaction methodologies are recommended to corroborate the anticipated structural and optical trends, specifically the band gap expansion and absorption characteristics. Photoluminescence and UV–Vis spectroscopy may offer direct evidence of the anticipated blue shift and improved charge carrier separation outlined in this study. In addition, more advanced computational methods, such as hybrid functional or GW-based methods, could be used to improve the analysis of the electronic structure and get better estimates of the band gap. These combined theoretical and experimental efforts would enhance the comprehension of Mg-doped $CaTiO_3$ and expedite its prospective application in high-efficiency solar and optoelectronic devices.

Author's Contribution: N.K & M.B.T., Conceived the idea; M.B.T. & B.A., Designed the simulated work or acquisition of data; B.A., Executed simulated work, data analysis or analysis and interpretation of data and wrote the basic draft; M.S, Did the language and grammatical edits or Critical revision

Funding: The publication of this article was funded by no one.

Conflicts of Interest: The authors declare no conflict of interest.

Acknowledgment: The authors would like to thank the advisors who advised for assistance with the collection of data.

References

1. Kannan, N., & Vakeesan, D. (2016). Solar energy for future world:-A review. *Renewable and sustainable energy reviews, 62*, 1092-1105. https://doi.org/10.1016/j.rser.2016.05.022
2. Holechek, J. L., Geli, H. M., Sawalhah, M. N., & Valdez, R. (2022). A global assessment: can renewable energy replace fossil fuels by 2050? *Sustainability, 14*(8), 4792. **https://doi.org/10.3390/su14084792**
3. Oberoi, A. S., Nijhawan, P., & Singh, P. (2018). A novel electrochemical hydrogen storage-based proton battery for renewable energy storage. *Energies, 12*(1), 82. **https://doi.org/10.3390/en12010082**
4. Soeder, D. J., & Soeder, D. J. (2021). Fossil fuels and climate change. *Fracking and the Environment: A scientific assessment of the environmental risks from hydraulic fracturing and fossil fuels*, 155-185. https://doi.org/10.1007/978-3-030-59121-2_9
5. Mitrašinović, A. M. (2021). Photovoltaics advancements for transition from renewable to clean energy. *Energy, 237*, 121510. https://doi.org/10.1016/j.energy.2021.121510
6. Reshak, A., Kogut, Y., Fedorchuk, A., Zamuruyeva, O., Myronchuk, G., Parasyuk, O., .Bila, J. (2013). Linear, non-linear optical susceptibilities and the hyperpolarizability of the mixed crystals Ag 0.5 Pb 1.75 Ge (S 1− x Se x) 4: experiment and theory. *Physical Chemistry Chemical Physics, 15*(43), 18979-18986. **https://doi.org/10.1039/C3CP53431F**
7. Reshak, A. H. (2014). Thermoelectric properties for AA-and AB-stacking of a carbon nitride polymorph (C 3 N 4). *RSC advances, 4*(108), 63137-63142. DOI: 10.1039/C4RA13342K

8. Kohn, W. and L. Sham, *Quantum density oscillations in an inhomogeneous electron gas.* Physical Review, 1965. **137**(6A): p. A1697.
9. Qiu, G., et al., *Theoretical study of the surface energy and electronic structure of pyrite FeS2 (100) using a total-energy pseudopotential method, CASTEP.* Journal of colloid and interface science, 2004. **270**(1): p. 127-132.
10. Ferhati, H., F. Djeffal, and F. AbdelMalek, *Towards improved efficiency of SnS solar cells using back grooves and strained-SnO2 buffer layer: FDTD and DFT calculations.* Journal of Physics and Chemistry of Solids, 2023. **178**: p. 111353.
11. Krause, A., et al., *Investigation of band gap and permittivity of the perovskite CaTiO3 in ultrathin layers.* Journal of Physics D: Applied Physics, 2015. **48**(41): p. 415304.
12. Vijatović, M., J. Bobić, and B.D. Stojanović, *History and challenges of barium titanate: Part I.* Science of Sintering, 2008. **40**(2): p. 155-165.
13. Rizwan, M., et al., *Effect of magnesium on structural and optical properties of CaTiO3: A DFT study.* Physica B: Condensed Matter, 2019. **568**: p. 88-91.

14. Luo, Q., et al., *Thermodynamics and kinetics of phase transformation in rare earth–magnesium alloys: A critical review.* Journal of Materials Science & Technology, 2020. **44**: p. 171-190.
15. Moreira, M.L., et al., *Structural and optical properties of CaTiO3 perovskite-based materials obtained by microwave-assisted hydrothermal synthesis: An experimental and theoretical insight.* Acta Materialia, 2009. **57**(17): p. 5174-5185.
16. Rizwan, M., et al., *Electronic and optical behaviour of lanthanum doped CaTiO3 perovskite.* Materials Research Express, 2020. **7**(1): p. 015920.
17. Wu, D., et al., *Effect of sintering temperature on structure and electrical transport properties of La0. 7Ca0. 26Na0. 04MnO3 ceramics.* Ceramics International, 2021. **47**(9): p. 12716-12724.
18. Hafez, A.M., N.M. Salem, and N.K. Allam, *Unravelling the correlated electronic and optical properties of BaTaO 2 N with perovskite-type structure as a potential candidate for solar energy conversion.* Physical Chemistry Chemical Physics, 2014. **16**(34): p. 18418-18424.
19. Rizwan, M., et al., *Photocatalytic and optical properties of (Mg: La) CaTiO3: Insights from first principles studies.* Journal of Physics and Chemistry of Solids, 2022. **169**: p. 110830.
20. Prasad, S., et al., *Solid-state mirrorless laser based on FRET system between two conjugated oligomers stability enhanced by MoS_2 nanosheets.* Journal of Materials Science: Materials in Electronics, 2025. **36**(29): p. 1-19.
21. Ayoub, I., et al., *Rare-earth-activated phosphors for LED applications*, in *Rare-Earth-activated Phosphors*. 2022, Elsevier. p. 205-240.
22. Lyu, M., D.-K. Lee, and N.-G. Park, *Effect of alkaline earth metal chloride additives BCl 2 (B= Mg, Ca, Sr and Ba) on the photovoltaic performance of FAPbI 3 based perovskite solar cells.* Nanoscale Horizons, 2020. **5**(9): p. 1332-1343.
23. Shanbhag, V.V., et al., *Comparative analysis of electrochemical performance and photocatalysis of SiO2 coated CaTiO3: RE3+ (Dy, Sm), Li+ core shell nano structures.* Inorganic Chemistry Communications, 2021. **134**: p. 108960.
24. Yang, H., et al., *The CdS/CaTiO3 cubic core-shell composite towards enhanced photocatalytic hydrogen evolution and photodegradation.* International Journal of Hydrogen Energy, 2023.
25. Oliveira, L.H., et al., *Investigation of structural and optical properties of CaTiO3 powders doped with Mg2+ and Eu3+ ions.* Journal of Alloys and Compounds, 2015. **647**: p. 265-275.
26. Guo, W., P. Zhao, and Z. Yue, *Modification of high-temperature electrical properties in CaTiO3 ceramics by Sm3+ and Al3+ doping.* Journal of Alloys and Compounds, 2023. **946**: p. 169389.
27. Aziz, S.B., et al., *Characteristics of PEO incorporated with CaTiO3 nanoparticles: structural and optical properties.* Polymers, 2021. **13**(20): p. 3484.

28. Hoat, D., J.R. Silva, and A.M. Blas, *First principles study of structural, electronic and optical properties of perovskites CaZrO3 and CaHfO3 in cubic phase.* Solid State Communications, 2018. **275**: p. 29-34.

29. Zhang, Q., et al. *A DFT Study on Electronic and Optical Properties of La/Ce-Doped CaTiO3 Perovskite*. in *International Conference on Energy Storage and Intelligent Vehicles*. 2022. Springer.